Theoretical study of the singlet and triplet vertical electronic transitions of styrene by the symmetry adapted cluster-configuration interaction method

Jian Wan [a,*], Hiroshi Nakatsuji [b,*]

[a] *Key Laboratory of Pesticide & Chemical Biology, College of Chemistry, Central China Normal University, Wuhan 430079, PR China*
[b] *Department of Synthetic Chemistry and Biological Chemistry, Graduate School of Engineering, Kyoto University, Sakyo-ku, Kyoto 606-8501, Japan*

Abstract

The ground state, singlet → singlet and singlet → triplet vertical excited states of styrene have been studied by using the symmetry adapted cluster-configuration interaction (SAC-CI) method with aug-cc-pVDZ basis sets supplemented with molecule-centered Rydberg functions. The characteristic structures of the bands observed in the vacuum ultraviolet (VUV) and electron energy loss (EEL) spectra have been theoretically clarified by calculating the excitation energies, oscillator strengths, and second moments for all the excited states in the energy region 2.6–7.0 eV. The present SAC-CI theoretical results, including both the singlet → singlet and singlet → triplet vertical electronic transitions, have well reproduced the profile of the electronic spectra of styrene. Higher-energy singlet → triplet excited states and Rydberg states were extensively addressed. The valence and Rydberg configurations were found strongly mix with each other in the $6^1A'$ and $8^1A'$ excited states at the SAC-CI/aug-cc-pVDZ(R) level. Three main differences were found comparing with the previous CASPT2 study. (1) The 3s'- and 3p-series of Rydberg states were predicted lower than the $5^1A'$ and $6^1A'$ valence π–π* excited states in the SAC-CI study, whereas higher than the $5^1A'$ and $6^1A'$ excited states in the CASPT2 study. (2) The valence excited state ($4^1A'$) involving doubly excited configurations $(4a'', 4a'') \rightarrow (5a'', 5a'')$ computed at 6.08 eV at the CASPT2 level was not found in the SAC-CI calculation. (3) The characterizations (main configurations) of the $5^1A'$ and $6^1A'$ excited states have been found to exchange their components in the SAC-CI and CASPT2 calculations.

1. Introduction

The electronic spectrum of styrene has been the subject of many theoretical and experimental studies [1–17]. It is not surprising since styrene is an interesting molecular system in which benzene ring conjugates with another unsaturated unit ethylene. Knowledge of the electronic states can lead to a more sophisticated understanding of the conjugation effect in different excited states. Furthermore, its electronic spectrum is nontrivial and contains many unresolved details, especially for the triplet and Rydberg transitions. Various types of experiments have been applied to extract information on

the spectrum [8–10,12], but a detailed assignment is extremely difficult because the presence of Rydberg series transitions overlap with valence transitions in the same energy region. Additionally, styrene is an ideal model system for studying photo-induced *cis–trans* isomerization process [15–17]. In comparison to stilbene, styrene is much more tractable for theoretical calculations because of its fewer electrons, which is certainly a merit in employing post-SCF methods.

Theoretical studies of the ground and excited states of styrene have been carried out by using semi-empirical and ab initio approaches [11–14]. The recent CASPT2 study [13] gave hitherto the highest theoretically calculated results (18 singlet → singlet and 2 singlet → triplet excited states) for the electronic excitations of styrene. To our surprise, there is so far no theoretical study on styrene based on the single reference coupled cluster

---

* Corresponding authors.
E-mail addresses: jianwan@mail.ccnu.edu.cn (J. Wan), hiroshi@sbchem.kyoto-u.ac.jp (H. Nakatsuji).

models such as SAC-CI [18–21], CCLR(CC2/3) [22–24], EOM-CC, and STOEM-CC [25–29].

In a recent series of SAC-CI (SD-R) studies [30–33], the singlet and triplet vertical excited states of cyclopentadiene [30], furan [31], pyrrole [31], thiophene [32], and pyridine [33] have been extensively investigated. The calculated excitation energies have been compared with experiments and other theoretical results including CASPT2, MRMP, ADC(2), EOM-CC, and CC2/CC3 methods [34–39]. Our results for both valence and Rydberg transitions were found systematically close to those of the CC2/3 level (within 0.2 eV). To further examine the efficiency and accuracy of SAC-CI (SD-R) method, in the present study, we did comparison and extensive study of the singlet and triplet vertical excited states of styrene at the SAC-CI/aug-cc-pVDZ(Ryd) level. In Section 2 we outline the computational details. Calculated results and discussions are presented in Section 3. A summary is given in Section 4.

2. Computational details

The details of the SAC-CI approach for calculating ground and excited states of molecules have been presented elsewhere [18–21,40–43]. Geometry optimizations with C_s symmetry were performed at B3LYP/6-31G(d,p) level [44], and the molecular plane was put on the xy-plane, and the calculated excitation energies are vertical in nature.

Most standard basis sets are optimized for ground-state calculations. Since excited states are often considerably more diffuse than ground states, extended basis sets are required. Therefore, we use well-extended basis sets to perform SAC-CI (SD-R) calculations: Dunning's augmented correlation consistent basis set aug-cc-pVDZ [45] was used for all carbon atoms, and cc-pVDZ [46] was used for all H atoms. A series of molecule-centered diffuse functions (3s3p3d) selected from the studies of Kaufmann et al. [47] was placed on the molecular center of gravity. In accordance with our previous experience, such basis sets should be well converged with respect to the number of Rydberg functions for at least for the 3s-, 3p-, and 3d-type Rydberg members [30–33]. Note that two s-, two p-, and two d-type diffuse functions [48] were placed at the charge centroid in the CASPT2 [13] study. All SCF calculations were performed with the Gaussian 98 package [49].

The present SAC-CI (SD-R) calculations were performed with the local version of the SAC-CI module [50]. The total number of basis functions is 270 at the HF/aug-cc-pVDZ (Ryd) level. The active space of SAC-CI (SD-R) calculation consists of the complete molecular orbital space (262) except that the innermost eight 1s core orbitals were frozen. All singlet and triplet excited states were calculated simultaneously with the same SAC ground-state energy as reference. In the SAC ground-state calculation, all single-excitation and selected double-excitation operators S_I^+ were included in the linked term. The energy threshold τ_g for the perturbation selection was 5.0×10^{-6} a.u. For the unlinked term, we included only the products of the double-excitation operators $S_I^+ S_J^+$ when the coefficients C_I and C_J, estimated by SD-CI in practice, were larger than 2.0×10^{-3}.

In the SAC-CI (SD-R) calculations of the excited states, all single-excitation operators and selected double-excitation operators were included in the linked operators R_K^+. The perturbation selection was performed as follows. First, we selected the main reference configurations from the SE-CI as those with a coefficient greater than 0.1, and then selected the double-excitation operator whose second-order perturbation energy with one of the main reference configurations is greater than the threshold τ_e (1.0×10^{-6} a.u.). In the unlinked term $\sum_{K,I} d_K C_I R_K^+ S_I^+ |0\rangle$, we included the double-excitation operators $\{S_I^+\}$ whose coefficients (C_I) were larger than 2.0×10^{-3} in the SAC ground-state calculation, and as the R_K^+ operator, we included single- and double-excitation operators whose coefficients (taken from SD-CI in practice) were greater than 0.05.

3. Results and discussion

3.1. Ground state geometry optimization

Geometry optimization for the ground state was performed at the B3LYP/6-31G(d,p) level. The resultant geometrical parameters are listed in Table 1. The labeling of the atoms in styrene is shown in Fig. 1.

Molina et al. [13] reported that the most pronounced effect of the nondynamic π electron correlation on the ground-state geometry of styrene occurs for the ethylenic double bond, and the π-CASSCF wave function yields a more reliable description of the ethylenic CC bond. The present results at the B3LYP/6-31G(d,p) level are consistent with those obtained at the π-CASSCF level [13] and the earlier predicted geometry [12].

3.2. Valence excited states

Some important molecular orbitals at the HF/aug-cc-pVDZ(Ryd) level were collected in Table 2. The highest two occupied MOs (HOMO and HOMO-1) are π orbitals in nature. In the unoccupied MOs, many Rydberg orbitals appear in the lower region and the valence π MOs appear in the energy region above 2.0 eV. The MOs 53 and 61 are the valence π orbitals in nature. The MO 58 is a Rydberg-valence mixed orbital. The MOs obtained at the HF/cc-pVDZ level (not including atom- and molecule-centered diffuse functions) are also shown

Table 1
Geometrical parameters obtained from full geometry optimization for the ground state of styrene

Parameter[a]	CASSCF Dunnig–Hay[b]	CASSCF ANO[c]	Present B3LYP(6-31G(d,p))	Predicted[d]
R(C1–C2)	1.349	1.346	1.343	1.340
R(C2–C3)	1.481	1.478	1.474	1.475
R(C3–C4)	1.409	1.406	1.411	1.406
R(C3–C5)	1.405	1.402	1.409	1.404
R(C4–C6)	1.397	1.394	1.395	1.393
R(C5–C7)	1.400	1.398	1.398	1.396
R(C6–C8)	1.402	1.400	1.402	1.399
R(C7–C8)	1.398	1.395	1.399	1.395
∠(C1C2C3)	127.4	127.5	127.6	
∠(C2C3C4)	123.1	123.1	123.1	
∠(C2C3C5)	118.8	118.8	118.8	

[a] Bond lengths in angstrom and angles in degrees.
[b] Dunning–Hay denotes C(9s5p1d)/[3s2p1d] and H(4s)/[2s] basis sets of Dunning and Hay.
[c] ANO denotes generally contracted basis sets of atomic natural orbitals: C(14s9p4d)/[3s2p1d] and H(8s)/[2s].
[d] The so-called predicted data obtained from ab initio calculations taking into account the deviations between experiment and theory for benzene and 1,3-butadiene.[16]
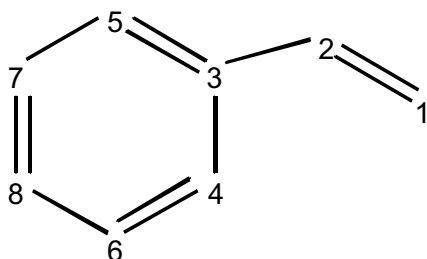

Fig. 1. Geometry and the numbering of atoms for styrene.

in Table 2. Albeit the excitation energies calculated at the SAC-CI/cc-pVDZ level is not accurate enough at all, the information such as the main configurations and energetic orders of the valence excited states of interest could be used as a comparison or reference in the following discussions.

The total SCF energy of styrene is calculated to be −307.618498 Hartree at the HF/aug-cc-pVDZ(Ryd) level. The SAC ground-state energy is −307.896036 Hartree at the SAC-CI/aug-cc-pVDZ(Ryd) level, and hence the calculated correlation energy is −0.277538 Hartree.

The valence and Rydberg transitions are distinguished by the criteria discussed in our previous studies [30–33] of five- and six-membered ring compounds. First, the A″ Rydberg states are not perturbed by the valence π–π* transitions. Second, the second moment of the charge distribution gives the size of the electron-cloud of the state under consideration. The main configuration, of course, gives the direct information about the nature of the excitation. In addition, the oscillator strength has been used as an indicator to distinguish valence and Rydberg states [34–39].

Fig. 2 is the schematic diagram of the highest two occupied and lowest three un-occupied π molecular orbital distributions of styrene at the HF/Aug-cc-pVDZ(Ryd) level. Since the single Hartree–Fock MOs were used as references in SAC-CI (SD-R) calculation, the distributions of these orbitals are useful for the analysis of the nature of the main configurations in the SAC-CI (SD-R) results. The calculated excitation energies for the singlet and triplet excited states by the SAC-CI (SD-R) method, together with the computed oscillator strengths, main configurations, second moments, and experimental data available, are collected in Table 3. The CASPT2 singlet and triplet excited states results [13] are also listed in Table 3 for comparison.

The EEL spectrum [12] in the energy range from 2.5 to 7.0 eV taken at an incident energy of 13.5 eV is shown at the top of Fig. 3. The first two triplet 0–0 transitions of styrene were observed at 2.69 and 3.98 eV. The present SAC-CI calculations computed seven triplet excited states below 6 eV and their energies are shown in the bottom of Table 3. The first two vertical triplet excited states, $1^3A'$ and $2^3A'$ were computed at 3.09 and 4.40 eV, respectively, which correspond to the first and second 0–0 transitions experimentally observed in this range. Both of them are valence excitations in nature, see Table 3 for detailed main configurations and assignments. CASPT2 calculated the lowest two triplet vertical excited states $1^3A'$ and $2^3A'$ at 3.03 and 4.09 eV, respectively. Note that the difference between SAC-CI (SD-R) and CASPT2 for the $2^3A'$ state is 0.31 eV. The other three triplet valence excited states in higher energy region were also predicted in the present SAC-CI (SD-R) calculation. The corresponding assignments were summarized in Table 3.

The CASPT2 study [13] reported that, for $1^3A'$ state, the ethylenic CC bond is elongated upon relaxation to nearly a single bond distance and the ethylene-phenyl link is significantly shortened. Such a change in the bond length is easily understood from the main configuration of the $1^3A'$ state and the associated orbital distributions

Table 2
Some important SCF occupied and unoccupied molecular orbitals (MOs) at HF/Aug-cc-pVDZ [3s4s5s/3p4p5p/3d4d5d] level

MOs		Symmetry	Orbital energy (eV)	Nature
Valence–Rydberg	Valence-only[a]			
Occupied				
27 (HOMO-1)	27	$3a''$	−9.2326	π
28 (HOMO)	28	$4a''$	−8.3063	π
Unoccupied [b]				
29 (LUMO)		a'	0.0493	s-Rydberg
30		a'	0.1616	p_x-Rydberg
31		a'	0.1657	p_y-Rydberg
32		a''	0.1837	p_z-Rydberg
33		a'	0.2074	s-Rydberg
34		a'	0.3420	d_{xx}-Rydberg
35		a'	0.3426	d_{yy}-Rydberg
36		a'	0.3608	d_{zz}-Rydberg
37		a''	0.3611	d_{xz}-Rydberg
38		a''	0.3614	d_{yz}-Rydberg
39		a'	0.4912	s-Rydberg
40		a'	0.5646	p_x-Rydberg
41		a'	0.5733	p_y-Rydberg
42		a''	0.6087	p_z-Rydberg
43		a'	0.9627	d_{yy}-Rydberg
44		a'	0.9644	d_{zz}-Rydberg
45		a'	1.0076	d_{xx}-Rydberg
46		a'	1.0144	s-Rydberg
47		a''	1.0196	d_{xz}-Rydberg
48		a''	1.0245	d_{yz}-Rydberg
49		a'	1.4438	p_x-Rydberg
50		a'	1.4972	p_y-Rydberg
51		a''	1.5424	p_z-Rydberg
52		a'	1.9054	s-Rydberg
53	29	$5a''$	2.0509	π
58		a''	2.5734	d_{yz}-Ryd-Valence mixed
61	30	$6a''$	2.9095	π

[a] Valence-only denotes the calculation was carried out by using 'bare' cc-pVDZ basis.
[b] The MOs 54–57, 59 and 60 are in Rydberg natures of d_{yy}, d_{zz}, d_{yy}, d_{xz}, p_x and d_{yy}.

given in Fig. 2. The $1^3A'$ state is described mainly by the singly excited configurations (28–53) and (28–58) with weights of 68% and 47%, respectively. The distribution of the virtual π MO 53 shows that there is no bonding contribution to the ethylenic CC bond; whereas there is a certain bonding-contribution to the ethylene-phenyl linking-bond. On the other hand, a strong bonding character in the ethylenic CC bond seen from the HOMO (28 MO) distribution is lost by this excitation.

The singlet–singlet transitions in the EEL spectrum were identified by a detailed comparison with the optical absorption spectrum. A low resolution, gas phase VUV spectrum (see the bottom of Fig. 3) shows three structureless bands with maxima at 4.42, 5.21, and 6.32 eV [8]. The exact positions of the 0–0 transitions to the first two singlet excited states have been determined by jet spectroscopy at 4.31 and 4.88 eV [9]. The maximum of the second intense band in the EEL spectrum is found at 5.00 eV [12]. Our present SAC-CI (SD-R) calculation gave 4.47 and 5.01 eV for the $2^1A'$ and $3^1A'$ singlet excited states with the cal-

culated intensities of 0.013 and 0.391, respectively. It is clear from the second moments shown in Table 3 that both of them are valence π–π^* transitions in nature. They are responsible for the first two bands of the gas phase VUV spectrum and the S_1 and S_2 peaks in the EEL spectrum shown in Fig. 3.

Note that the EEL spectroscopy study [12] assumed that two singlet → singlet valence excited states are involved in the second intense band (band II), however, our present SAC-CI results and CASPT2 results do not support this assumption. Only one singlet valence π–π^* excited state with strong intensity occurs in the second intense band. Beside the contribution of the vibrational structures of the valence excitation, one possible explanation of the second intense band in EEL spectrum from the present SAC-CI results is to attribute it to the third and forth triplet excitations, $3^3A'$ and $4^3A'$, calculated at 4.51 and 4.92 eV, respectively, which are valence excitations in nature. Actually, the second band in the low-resolution VUV spectrum [8] of gas phase is not very intense.
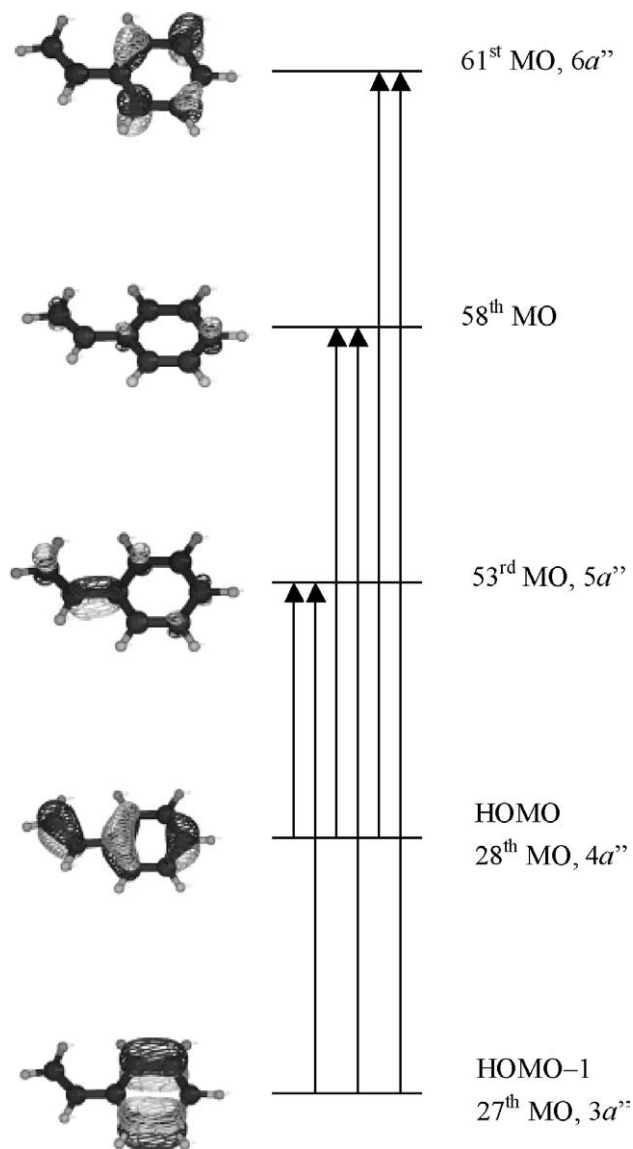
Fig. 2. Schematic diagram showing the highest two occupied and lowest three unoccupied π molecular orbital distribution of styrene at HF/Aug-cc-pVDZ(Ryd) level.
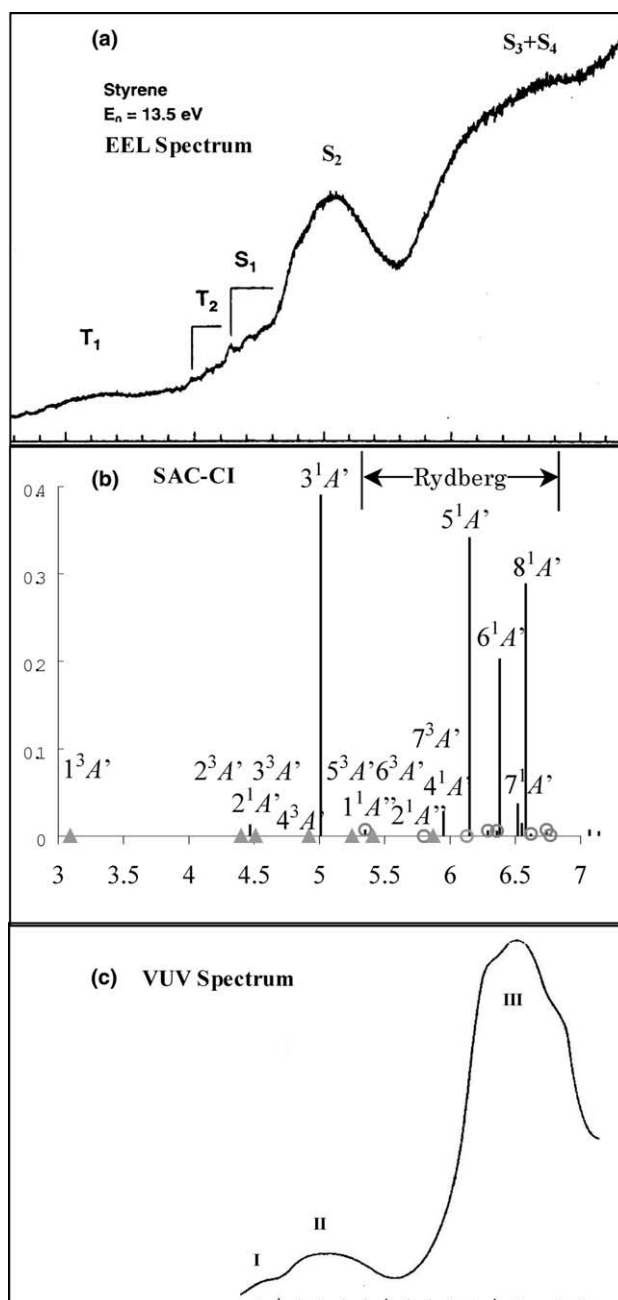

Fig. 3. (a) Experimental EEL spectrum [12], (b) SAC-CI vertical excited states, and (c) experimental VUV [8] spectrum of styrene (triangle mark denotes triplet state, circle mark denotes the Rydberg excited state with small oscillator strength, see Table 3 for the detailed assignments).

The previous experimental studies together with the theoretically predicted excitation energies suggested a possible existence of an effective path for the intersystem crossing (ISC) through higher triplet excited states [12,51,52]. The present SAC-CI (SD-R) results showed that the second triplet state is somewhat lower in energy than the first singlet excited state, hence giving further support to the possible existence of an effective channel for the ISC.

At higher energy range, the EEL spectrum [12] shows a most broad and intense band (third band) without distinct maximum. Swiderek and coworkers [12] suggested that this band must be at least partly related to the strongest and broad band of the gas-phase VUV spectrum [8] with a maximum at 6.32 eV. Our present

SAC-CI (SD-R) calculations gave a lot of singlet → singlet excited states in this energy region. Among them three singlet → singlet excited states $5^1A'$, $6^1A'$, and $8^1A'$ were predicted at 6.15, 6.38, and 6.58 eV with stronger oscillator strengths of 0.342, 0.203, and 0.289, respectively. They are certainly in the energy region of the strongest broad band (band III) of the gas-phase VUV spectrum (see the bottom of Fig. 3) and should be responsible for this band in the gas phase VUV spec-

trum and for the strongest intense and broad band in the EEL spectrum (see the top of Fig. 3). From the second moments and the main configurations listed in Table 3, one can see that two of three singlet excited states, $5^1A'$ and $6^1A'$, are valence excitations showing more or less diffuse characters due to mixing of the Rydberg states. The $6^1A'$ and $8^1A'$ states can be described as linear combination of the $27 \to 61$ and $28 \to 3d$-Ryd one-electron configurations. The interaction between them leads to a valence state (S.M. 184.7 a.u.) and a Rydberg state (S.M. 227.8 a.u.) at 6.38 and 6.58 eV, respectively. Frankly, It is hard to completely distinguish the nature of $6^1A'$ and $8^1A'$ states from the main configurations, oscillator strengths, and second moments. We tentatively made the above assignment taking into account the energy gain (0.16 and 0.11 eV) of the two higher valence excited states obtained at the SAC-CI/cc-pVDZ and CASPT2 level. According to our present calculation and assignment, the interval between $5^1A'$ and $6^1A'$ states is 0.23 eV, whereas that of CASPT2 is 0.11 eV. Considering the energy gain and the superposition of the intensities of $5^1A'$, $6^1A'$, and $8^1A'$ three excited states, the present SAC-CI (SD-R) results could give a satisfactory description of the strongest intense and broad band in the experimental VUV and EEL spectra.

An interesting and important issue is the characterization of the strongest broad absorption band in gasphase VUV spectrum. Our present calculated results and characterizations are different from those of the CASPT2 study, albeit two results coincide with that the bulk of the intensity of the band arising from the two higher π–π^* intra-valence transitions.

The main configurations of the individual excited state listed in Tables 3 and 4 show that the $2^1A'$ valence excited state is composed of $4a'' \to 6a''$ and $3a'' \to 5a''$, and the $3^1A'$ valence excited state is composed of $4a'' \to 5a''$ and $3a'' \to 5a''$ (see Table 2 for the definition of $3a''$, $4a''$, $5a''$, and $6a''$). The CASPT2 study gave almost the same principle configurations for the lowest two valence excited states. However, a valence excited state $(4^1A')$ involving doubly excited configurations $(4a'', 4a'') \to (5a'', 5a'')$ computed at 6.08 eV with a weak intensity of 0.002 at the CASPT2 level was not found in the SAC-CI (SD-R) calculation. The $4^1A'$ state was computed at 5.95 eV with an intensity of 0.0282 at the SAC-CI/aug-cc-pVDZ(Ryd) level and assigned to the $3p_z$-Rydberg nature. This difference should be further investigated in the future theoretical study, which may be an example again shows that CASPT2 and single-reference coupled cluster models are in some sense complementary.

Furthermore, the main configurations of $5^1A'$ state computed at 6.15 eV in SAC-CI are $4a'' \to 6a''$ and $3a'' \to 5a''$, which is totally different from $3a'' \to 6a''$ of $5^1A'$ state computed at 6.19 eV in the CASPT2 study. The main configurations of the $6^1A'$ state computed at

6.38 eV in SAC-CI are $3a'' \to 6a''$ and some Rydberg transitions, which is also different from $4a'' \to 6a''$ and $3a'' \to 5a''$ of $6^1A'$ state computed at 6.3 eV at the CASPT2 level. From the above comparison of main configurations, one can see that the $5^1A'$ state of SAC-CI is actually corresponding to the $6^1A'$ state of CASPT2, and the $6^1A'$ state of SAC-CI is actually corresponding to the $5^1A'$ state of CASPT2. In other words, the characterizations (main configurations) of the two higher valence π–π^* excited states ($5^1A'$ and $6^1A'$) exchange positions in the SAC-CI and CASPT2 calculations.

From Tables 3 and 4, one can see that the main configurations of all four valence excited states and their corresponding energy orders are very similar at the SAC-CI/aug-cc-pVDZ(Ryd) and SAC-CI/cc-pVDZ levels, i.e., with and without atom- and molecule-centered diffuse functions. It shows that taking into account the diffuse functions in the SAC-CI calculation does not cause the energy order and main configurations of the valence excited states to change dramatically.

3.3. Rydberg excited states

The present SAC-CI (SD-R) calculations also gave an extensive prediction of the Rydberg states in the energy region of interest. The available experimental data on Rydberg states are not much for styrene, which makes it difficult to compare the theoretical results with the experimental data. Nevertheless, the present theoretical results on the Rydberg transitions are expected to be helpful for the future experimental spectroscopic studies of styrene.

The Rydberg transitions originating out of the $4a''$ orbital (HOMO) are substantially different from those originating from the $3a''$ orbital (HOMO-1). For convenience, the series of Rydberg states exciting out of $4a''$ orbital are labeled as ns-, np- and nd-Ryd. ($n = 3$ and 4), and those exciting out of $3a''$ orbital are labeled as ns'- and np'-Ryd. ($n = 3$).

The first singlet Rydberg state, $1^1A''$ ($4a'' \to 3s$-Ryd), was computed at 5.35 eV at SAC-CI/aug-cc-pVDZ level. The CASPT2 study computed the ($4a'' \to 3s$-Ryd) state at 5.85 eV. The $2^1A''$ ($4a'' \to 3p_x$-Ryd), $3^1A''$ ($4a'' \to 3p_y$-Ryd), and $4^1A'$ ($4a'' \to 3p_z$-Ryd) states were computed at 5.74, 5.80, and 5.95 eV, respectively, at the SAC-CI/aug-cc-pVDZ level. The CASPT2 study computed the ($4a'' \to 3p_y$-Ryd) state at 6.35 eV, the ($4a'' \to 3p_x$-Ryd) state at 6.36 eV, and the ($4a'' \to 3p_z$-Ryd) state at 6.50 eV.

The main configurations of the $4^1A''$ state: $27 \to 39$, $27 \to 52$, and $27 \to 33$, clearly shows that it is the excitation from the $3a''$ orbital to the 3s-Rydberg orbitals. The $4^1A''$ state ($3a'' \to 3s'$-Ryd) was computed at 6.13 eV at the SAC-CI/aug-cc-pVDZ level. The CASPT2 study computed the ($3a'' \to 3s'$-Ryd) state at 6.38 eV.

Note that the 3s'- and 3p-series of Rydberg transitions were predicted lower than the $5^1A'$ and $6^1A'$

Table 3
SAC-CI results for the singlet and triplet excited states of styrene compared with CASPT2 results and experimental data[a]

State	Nature	Main configuration	SAC-CI			CAS-PT2		Experimental[b]
			S.M.	OSC	ΔE	ΔE	OSC	
$1^1A'$	G.S.		106.4	0.0	0.0			
$2^1A'$	Valence	$-0.56(28–61) − 0.43(27–53) + 0.32(27–58) − 0.28(28–53)$	107.5	0.0133	4.47	4.34	0.001	4.42 (0.02)
$3^1A'$	Valence	$-0.68(28–53) + 0.37(28–58) − 0.33(28–51) + 0.21(27–53)$	114.8	0.3907	5.01	4.97	0.316	5.21 (0.24)
$1^1A''$	3s-Ryd.	$-0.42(28–33) + 0.41(28–39) + 0.38(28–52) − 0.36(28–46)$	167.9	0.0072	5.35	5.85	0.004	
$2^1A''$	$3p_x$-Ryd.	$0.50(28–49) − 0.42(28–40) − 0.38(28–30) − 0.31(28–41)$	190.5	0.0001	5.74	6.36	0.001	
$3^1A''$	$3p_y$-Ryd.	$0.50(28–50) + 0.48(28–41) + 0.41(28–31) − 0.41(28–40)$	212.0	0.0000	5.80	6.35	0.000	
$4^1A'$	$3p_z$-Ryd.	$-0.60(28–42) + 0.45(28–51) − 0.38(28–32) − 0.29(28–53)$	192.0	0.0282	5.95	6.50	0.005	
$4^1A''$	3s'-Ryd.	$0.40(27–39) + 0.39(27–52) − 0.38(27–33) − 0.33(27–46)$	170.8	0.0000	6.13	6.38	0.000	
$5^1A'$	Valence	$0.61(28–61) − 0.38(27–53) − 0.31(27–51) + 0.28(27–58)$	124.9	0.3416	6.15	6.3	0.247	6.20
$5^1A''$	$3d_{xx}$-Ryd.	$-0.40(28–43) + 0.38(28 − 45) − 0.36(28–35) − 0.33(28–44)$	248.5	0.0063	6.29	7.00	0.000	
$6^1A''$	$3d_{yy}$-Ryd.	$-0.51(28–43) + 0.46(28–34) + 0.36(28–44) − 0.34(28–54)$	242.3	0.0003	6.32	7.00	0.000	
$7^1A''$	$3d_{zz}$-Ryd.	$-0.45(28–44) + 0.36(28–46) − 0.33(28–35) − 0.33(28–55)$	230.4	0.0059	6.36	7.10	0.000	
$6^1A'$	V-Ryd.	$0.54(27–61) − 0.46(28–47) − 0.38(28–38) + 0.25(28–58)$	184.7	0.2026	6.38	6.19	0.691	6.32
$7^1A'$	$3d_{xz}$-Ryd.	$0.61(28–48) + 0.57(28–37) − 0.29(28–57)$	266.8	0.0373	6.52	6.79	0.071	
$8^1A''$	$3p_x$-Ryd.	$0.52(27–49) − 0.47(27–40) − 0.35(27–30) + 0.30(27–39)$	198.0	0.0146	6.55			
$8^1A''$	$3d_{yz}$-Ryd-V	$0.54(27–61) + 0.49(28–38) + 0.36(28–47) + 0.22(27–53)$	227.9	0.2888	6.58	7.09	0.012	6.57
$9^1A''$	4s-Ryd.	$-0.57(28–29) + 0.44(28–33) − 0.38(28–45) + 0.28(28–52)$	428.7	0.0026	6.62			
$10^1A''$	$4p_x$-Ryd.	$0.80(28–30) + 0.43(28–49)$	514.3	0.0001	6.72			
$9^1A'$	$4p_z$-Ryd.	$0.61(28–32) + 0.36(27–42) + 0.33(28–51) − 0.30(27–51)$	377.8	0.0071	6.74			
$11^1A''$	$4p_y$-Ryd.	$-0.81(28–31) + 0.44(28–50)$	550.1	0.0000	6.75			
$10^1A'$	$3p_z$-Ryd.	$-0.53(28–32) + 0.42(27–42) − 0.33(27–51) − 0.30(28–51)$	335.2	0.0009	6.77			
$11^1A'$	$4d_{yz−xy}$-Ryd.	$-0.52(28–37) − 0.47(28–38) + 0.38(28–47) − 0.26(28–58)$	516.7	0.0072	7.07			
$12^1A'$	$4d_{xy−yz}$-Ryd.	$-0.48(28–37) + 0.39(28–48) + 0.27(28–65) + 0.26(26–53)$	416.1	0.0054	7.14			
$1^3A'$	Valence	$-0.68(28–53) + 0.47(28–58)$	106.8	–	3.09	3.03	–	2.69[c]
$2^3A'$	Valence	$0.50(27–61) − 0.47(27–53) + 0.24(28–61)$	107.0	–	4.40	4.09	–	3.98[c]
$3^3A'$	Valence	$0.57(28–61) + 0.49(27–61)$	107.2	–	4.51			
$4^3A'$	Valence	$0.48(26–53) − 0.35(27–61)$	108.1	–	4.92			
$5^3A'$	Valence	$0.54(28–61) + 0.48(27–53) − 0.24(27–61)$	109.2	–	5.25			
$1^3A''$	3s-Ryd.	$0.42(28–33) − 0.41(28–39)$	167.9	–	5.41			
$2^3A''$	$3p_y$-Ryd.	$-0.57(28–41) − 0.52(28–50)$	213.0	–	5.87			

Experimental column additional values: 6.32 (2.4) grouped with 5A', 6A' (6.20), and 6.57 (8A'').

[a] S.M. and OSC denote second moment and oscillator strength, respectively.

[b] Values in parentheses are the experimental f values obtained from the integral areas under the absorption curves by the use of the following equation $f = 4.32 \times 10^{-9} \int \varepsilon \, dv$, where ε is the molar extinction coefficient and v is the frequency in cm^{-1} (see [14]).

[c] The position of the 0–0 transition (see [16]).

Table 4
SAC-CI results for the valence excitations of styrene using 'bare' cc-pVDZ basis set that does not include atom-centered and molecule-centered Rydberg functions

State	Nature	Main configurations[a]	S.M.	OSC	ΔE
$1^1A'$	G.S.		103.9		
$2^1A'$	Valence	$0.63(27–29) - 0.63(28–30) + 0.16(28–29)$	104.6	0.0044	5.01
$3^1A'$	Valence	$0.92(28–29) + 0.19(27–30) - 0.18(27–29)$	105.2	0.5209	5.90
$4^1A'$	Valence	$0.68(28–30) + 0.62(27–29) + 0.19(27–30)$	104.3	0.4488	7.19
$5^1A'$	Valence	$-0.80(27–30) + 0.44(26–29) + 0.19(28–29)$	103.9	0.6531	7.35
$6^1A'$	Valence	$0.60(26–29) + 0.56(28–34) + 0.30(27–30)$	105.6	0.0938	7.58
$7^1A'$	Valence	$0.70(26–30) + 0.44(27–34) - 0.15(27–29)$	103.2	0.0443	8.42
$8^1A'$	Valence	$-0.71(28–34) + 0.49(26–29) + 0.31(27–30)$	105.6	0.2712	8.79
$1^3A'$	Valence	$0.89(28–29) - 0.26(26–34) + 0.24(27–30)$	104.3	–	3.69
$2^3A'$	Valence	$0.76(27–30) - 0.34(26–29) - 0.32(27–29)$	104.2	–	4.95
$3^3A'$	Valence	$0.64(28–30) + 0.59(27–29) + 0.29(27–30)$	104.4	–	5.11
$4^3A'$	Valence	$0.63(26–29) - 0.52(28–34) + 0.43(27–30)$	104.4	–	5.46
$5^3A'$	Valence	$-0.66(28–30) + 0.65(27–29) + 0.17(26–30)$	104.6	–	6.07

[a] The MO number is given in Table 2.

valence π–π* excited states in the SAC-CI (SD-R) calculation, but were predicted higher than the $5^1A'$ and $6^1A'$ valence π–π* excited states in the CASPT2 calculation. Moreover, the energy difference for the 3s- and 3p-series of Rydberg states is over 0.5 eV between the SAC-CI and CASPT2 calculations. In all previous theoretical studies of furan, pyrrole, thiophene, pyridine, and benzene molecules, the case of the 3p-series of Rydberg transitions were predicted over all four valence π–π* excitations is not found. It is an interesting finding and deserves to be investigated in further theoretical and experimental comparison studies.

The 3d-, 4s-, 4p-, and 3p′-series Rydberg states were theoretically predicted within the energy range of 6.1–7.2 eV (see Table 3 for details). In addition, two triplet Rydberg states, $1^3A''$ (3s-Ryd) and $2^3A''$ (3p$_y$-Ryd), were computed at 5.41 and 5.87 eV, respectively.

The accuracy of the present SAC-CI (SD-R) Rydberg excitation energies are expected to be within 0.2 eV deviations according to the experiences obtained from our previous theoretical investigations [30–33]. Note that two s-, two p-, and two d-type diffuse functions [48] were placed at the charge centroid in the CASPT2 [13] study.

3.4. Valence–Rydberg interaction

In order to investigate the effect of Rydberg functions on the valence excitations, a comparative calculation was carried out using 'bare' cc-pVDZ basis set, which is referred as to a valence-only calculation. The computational details are the same as those in the previous one (see Section 2); except that the atom-centered diffuse functions and molecule-centered Rydberg functions were deleted. The character of the MOs near the HOMO–LUMO region is given in Table 2 in comparison with those of the valence–Rydberg calculations. The excitation energies, main configurations, second mo-

ments, and oscillator strengths of the pure valence excitations of interest are collected in Table 4.

Comparing the valence excitations given in the Table 3 with the corresponding data in Table 4, one can see the effect of Rydberg functions on the excitation energies, second moments, and oscillator strengths of the valence excitations in styrene. First, an inclusion of the appropriate Rydberg functions dramatically decreases the excitation energies of both singlet and triplet excited states. Second, the Rydberg functions have a larger influence on the second moments of the singlet states than that of the triplet states. When valence–Rydberg mixing occurs, the associated second moment becomes larger. The larger the interaction between valence and Rydberg is, the larger the second moment is. Without Rydberg functions, the second moments of all calculated valence excitations are almost the same, as seen in Table 4, as the second moment of the ground state. However, in Table 3, the second moments of the valence excitations $2^1A'$, $3^1A'$, $5^1A'$, and $6^1A'$ are 107.5, 114.8, 124.9, and 184.7, respectively, which are very different from each other. This trend showed that the interaction between valence and Rydberg basis becomes stronger and stronger as the energy becomes higher, especially in the third strongest broad band: actually, a number of Rydberg excitations were theoretically predicted in this energy region. The oscillator strengths of the singlet valence excited states also changed as the Rydberg functions were taken into account. Note that without Rydberg functions, the $5^1A'$ valence excitation has the largest oscillator strength. After considering the Rydberg functions, the oscillator strengths of all the valence excitations, including the valence–Rydberg mixed states, become smaller, though they still retain relatively strong intensities.

For the triplet states, the valence–Rydberg mixing is smaller than that for the singlet states, as clearly seen

from the S.M. shown in Table 3. However, the excitation energy calculated from the valence-only basis set is much higher than those with the valence–Rydberg mixed basis set and does not explain the experimental values. Thus, the Rydberg basis is also important for calculating the triplet excited states of styrene.

Another issue deserves to be pointed out is that there exist stronger mixings of valence and Rydberg main configurations in the $6^1A'$ and $8^1A'$ excited states at the SAC-CI/aug-cc-pVDZ(Ryd) level. The above two excited states can be described as a linear combination of the $27 \rightarrow 61$ and $28 \rightarrow$ 3d-Ryd one-electron configurations. The interaction between them leads to a valence state $6^1A'$ (S.M. 184.7 a.u.) and a Rydberg state $8^1A'$ (S.M. 227.8 a.u.) at 6.38 and 6.58 eV, respectively. Thus, an attempt to assign pure valence or pure Rydberg excitations for these two excited states is meaningless. In our present calculations, we found that one valence transition configuration $27 \rightarrow 61$ is included in both $6^1A'$ and $8^1A'$ excited states, and its contributions (absolute value of the coefficient of configuration) to the $6^1A'$ and $8^1A'$ states are the same 54%. This further shows that the intensity of this energy region can be attributed mostly to this valence transition configuration.

4. Concluding remarks

In the present study, the singlet and triplet valence and Rydberg vertical excited states of styrene were theoretically investigated by the SAC-CI (SD-R) method with an extended basis set and a large active orbital space. The 22 low-lying singlet and 7 triplet excited states were calculated, and a reliable assignment of the VUV and EEL spectra up to 7 eV was made using the calculated excitation energies and the associated oscillator strengths and second moments.

The first and second singlet valence π–π^* excited states, $2^1A'$ and $3^1A'$, were computed at 4.47 and 5.01 eV with the oscillator strengths of 0.013 and 0.391, respectively, and are assigned to the first band of the VUV and EEL spectra. The $5^1A'$ and $6^1A'$ valence π–π^* excited states computed at 6.15 and 6.38 eV with the oscillator strengths of 0.3416 and 0.2026 are responsible for the third strongest broad band of the VUV spectrum and EEL spectrum.

The first two lowest triplet valence excited states, $1^3A'$ and $2^3A'$, were assigned to the experimentally observed T_1 and T_2 states of the EEL spectrum. The contribution of the higher triplet valence excited states, $3^3A'$, $4^3A'$, and $5^3A'$, calculated at 4.51, 4.92, and 5.25 eV should also be important for the EEL spectrum.

Three main differences were found comparing with the previous CASPT2 study. The 3s′- and 3p-series of Rydberg states were predicted lower than the $5^1A'$ and $6^1A'$ valence π–π^* excited states in the SAC-CI study,

whereas higher than the $5^1A'$ and $6^1A'$ excited states in the CASPT2 study. The valence excited state ($4^1A'$) involving doubly excited configurations $(4a'',4a'') \rightarrow (5a'', 5a'')$ computed at 6.08 eV at the CASPT2 level was not found in the SAC-CI calculation. The characterizations (main configurations) of the $5^1A'$ and $6^1A'$ excited states have been found to exchange positions in the SAC-CI and CASPT2 calculations.

References

[1] M.C. Bruni, F. Momicchioli, I. Baraldi, J. Langlet, Chem. Phys. Lett. 36 (1975) 484.
[2] G.L. Bandazzoli, G. Orlandi, P. Palmieri, G. Poggi, J. Am. Chem. Soc. 100 (1978) 392.
[3] G. Orlandi, P. Palmieri, G. Poggi, J. Chem. Soc., Faraday Trans. II 77 (1981) 71.
[4] I. Nebot-Gil, J.-P. Malrieu, Chem. Phys. Lett. 84 (1981) 571.
[5] M. Said, J.-P. Malrieu, Chem. Phys. Lett. 102 (1983) 312.
[6] M.J. Bearpark, M. Olivucci, S. Wilsey, F. Bernardi, M.A. Robb, J. Am. Chem. Soc. 117 (1995) 6944.
[7] J.A. Syage, P.M. Felker, A.H. Zewail, J. Chem. Phys. 81 (1984) 4706.
[8] K. Kimura, S. Nagakura, Theoret. Chim. Acta 3 (1965) 164.
[9] D.G. Leopold, R.J. Hemley, V. Vaida, J.L. Roebber, J. Chem. Phys. 75 (1981) 4758.
[10] T.Ni.R.A. Caldwell, I.A. Melton, J. Am. Chem. Soc. 111 (1989) 457.
[11] R.J. Hemley, U. Dinur, V. Vaida, M. Karplus, J. Am. Chem. Soc. 107 (1985) 836.
[12] P. Swiderek, M.-J. Fraser, M. Michaud, L. Sanche, J. Chem. Phys. 100 (1994) 70.
[13] V. Molina, B.R. Smith, M. Merchan, Chem. Phys. Lett. 309 (1999) 486.
[14] V. Molina, M. Merchan, B.O. Roos, P. Malmqvist, Phys. Chem. Chem. Phys. 2 (2000) 2211.
[15] M.H. Hui, S.A. Rice, J. Chem. Phys. 61 (1974) 833.
[16] J.M. Hollas, T. Ridley, J. Mol. Spectrosc. 89 (1981) 232.
[17] J.A. Syage, F. al Adel, A.H. Zewail, Chem. Phys. Lett. 103 (1983) 15.
[18] H. Nakatsuji, K. Hirao, J. Chem. Phys. 68 (1978) 2053.
[19] H. Nakatsuji, Chem. Phys. Lett. 59 (1978) 362.
[20] H. Nakatsuji, Chem. Phys. Lett. 67 (1979) 329.
[21] H. Nakatsuji, in: Computational Chemistry: Reviews of Current Trends, vol. 2, edited.
[22] H. Koch, P. Jorgensen, J. Chem. Phys. 93 (1990) 3333.
[23] O. Christiansen, H. Koch, P. Jorgensen, J. Olsen, Chem. Phys. Lett. 256 (1996) 185.
[24] O. Christiansen, J. Gauss, J. Stanton, P. Jørgensen, J. Chem. Phys. 111 (1999) 525.

[25] H. Sekino, R.J. Bartlett, Int. J. Quantum Chem. Symp. 18 (1984) 255.

[26] J.F. Stanton, R.J. Bartlett, J. Chem. Phys. 98 (1993) 7029.

[27] M. Nooijen, R.J. Bartlett, J. Chem. Phys. 106 (1997) 6441.

[28] M. Nooijen, R.J. Bartlett, J. Chem. Phys. 106 (1997) 6449.

[29] M. Nooijen, R.J. Bartlett, J. Chem. Phys. 107 (1997) 6812.

[30] J. Wan, M. Ehara, M. Hada, H. Nakatsuji, J. Chem. Phys. 113 (2000) 5245.

[31] J. Wan, J. Meller, M. Hada, M. Ehara, H. Nakatsuji, J. Chem. Phys. 113 (2000) 7853.

[32] J. Wan, M. Hada, M. Ehara, H. Nakatsuji, J. Chem. Phys. 114 (2001) 842.

[33] J. Wan, M. Ehara, M. Hada, H. Nakatsuji, J. Chem. Phys. 114 (2001) 5117.

[34] M.H. Palmer, I.C. Walker, C.C. Ballard, M.F. Guest, Chem. Phys. 192 (1995) 111.

[35] M.H. Palmer, I.C. Walker, M.F. Guest, Chem. Phys. 238 (1998) 179.

[36] M.H. Palmer, I.C. Walker, M.F. Guest, Chem. Phys. 241 (1999) 275.

[37] A.B. Trofimov, J. Schirmer, Chem. Phys. 214 (1997) 153.

[38] A.B. Trofimov, J. Schirmer, Chem. Phys. 224 (1997) 175.

[39] L. Serrano-Andres, M. Merchan, I. Nebot-Gil, B.O. Roos, M.P. Fulscher, J. Am. Chem. Soc. 115 (1993) 6184.

[40] K. Hirao, H. Nakatsuji, Chem. Phys. Lett. 79 (1981) 292.

[41] H. Nakatsuji, Chem. Phys. 75 (1983) 425.

[42] H. Nakatsuji, Chem. Phys. Lett. 177 (1991) 331.

[43] H. Nakatsuji, J. Chem. Phys. 83 (1985) 5743.

[44] A.D. Becke, in: D.R. Yarkony (Ed.), Modern Electronic Structure Theory Part II, World Scientific, Singapore, 1995.

[45] R.A. Kendall, T.H. Dunning Jr., R.J. Harrison, J. Chem. Phys. 96 (1992) 6796.

[46] T.H. Dunning Jr., J. Chem. Phys. 90 (1989) 1007.

[47] K. Kaufmann, W. Baumeister, M. Jungen, J. Phys. B 22 (1989) 2223.

[48] M. Rubio, M. Merchan, E. Orti, B.O. Roos, Chem. Phys. 179 (1994) 395.

[49] Gaussian 98 (Revision A.1), M.J. Frisch, G.W. Trucks, H.B. Schlegel, G.E. Scuseria, M.A. Robb, J.R. Cheeseman, V.G. Zakrzewski, J.A. Montgomery, R.E. Stratmann, J.C. Burant, S. Dapprich, J.M. Millam, A.D. Daniels, K.N. Kudin, M.C. Strain, O. Farkas, J. Tomasi, V. Barone, M. Cossi, R. Cammi, B. Mennucci, C. Pomelli, C. Adamo, S. Clifford, J. Ochterski, G.A. Petersson, P.Y. Ayala, Q. Cui, K. Moro-kuma, D.K. Malick, A.D. Rabuck, K. Raghavachari, J.B. Foresman, J. Cioslowski, J.V. Ortiz, B.B. Stefanov, G. Liu, A. Liashenko, P. Piskorz, I. Komaromi, R. Gomperts, R.L. Martin, D.J. Fox, T. Keith, M.A. Al-Laham, C.Y. Peng, A. Nanayakkara, C. Gonzalez, M. Challacombe, P.M.W. Gill, B.G. Johnson, W. Chen, M.W. Wong, J.L. Andres, M. Head-Gordon, E.S. Replogle, J.A. Pople, Gaussian, Inc., Pittsburgh PA, 1998.

[50] H. Nakatsuji, M. Hada, M. Ehara, J. Hasegawa, T. Nakajima, H. Nakai, O. Kitao, K. Toyota, SAC/SAC-CI program system (SAC-CI96) for calculating ground, excited, ionized, and electron attached states and singlet to septet spin multiplicities.

[51] V. Molina, M. Merchan, B.O. Ross, Spectrochim. Acta A 55 (1999) 433.

[52] V. Molina, M. Merchan, B.O. Ross, Per-Ake Malmqvist, Phys. Chem. Chem. Phys. 2 (2000) 2211.